AJNR

Brain Fluorine-18 Fluorodeoxyglucose Imaging with Dual-Head Coincidence Gamma Camera:Comparison with Dedicated Ring-Detector PositronEmission Tomography

Kazuki Fukuchi, Kohei Hayashida, Hiroshi Moriwaki, Kazuhito Fukushima, Norihiko Kume, Tetsuro Katafuchi, Masayoshi Sago, Makoto Takamiya and Yoshio Ishida

AJNR Am J Neuroradiol 2000, 21 (1) 99-104
http://www.ajnr.org/content/21/1/99

AJNR Am J Neuroradiol 21:99–104, January 2000

Brain Fluorine-18 Fluorodeoxyglucose Imaging with Dual-Head Coincidence Gamma Camera: Comparison with Dedicated Ring-Detector Positron Emission Tomography

Kazuki Fukuchi, Kohei Hayashida, Hiroshi Moriwaki, Kazuhito Fukushima, Norihiko Kume, Tetsuro Katafuchi, Masayoshi Sago, Makoto Takamiya, and Yoshio Ishida

BACKGROUND AND PURPOSE: **Dual-head coincidence gamma camera (DHC) imaging has been proposed as an alternative to dedicated ring-detector positron emission tomography (dr-PET) for clinical fluorodeoxyglucose (FDG) studies. The purpose of this investigation was to assess the quality of DHC images in FDG studies of the human brain.**

METHODS: **Seven healthy volunteers and 12 patients with various cerebral disorders underwent consecutive brain dr-PET and DHC with FDG. All sets of images were compared semiquantitatively using regions of interest.**

RESULTS: **Cortical count ratios to the cerebellum on DHC and dr-PET images did not differ significantly among the volunteers, except in the superior frontal cortex and thalamus. In all studies including those of cerebral disorders, the mean cortical-to-cerebellar ratios of DHC and dr-PET images correlated closely.**

CONCLUSION: **FDG imaging with DHC delineated the metabolic distribution of glucose in the brain as well as dr-PET did, except in the superior frontal cortex and thalamus. Therefore, DHC may be a dedicated cost-effective means of detecting metabolic abnormalities in the brain.**

Positron emission tomography (PET) with fluorine-18 fluorodeoxyglucose (FDG) is useful to diagnose and manage patients with seizure, brain tumor, or dementia (1–3). The use of PET as a clinical imaging technique is limited because of the high costs associated with managing and purchasing the PET camera system, a cyclotron, and the support laboratory (4). Thus, the discovery of alternative, cost-effective methods of imaging 511-keV photons released by positron emitters is desirable.

Dual-head coincidence gamma camera (DHC) imaging has been proposed as a means of acquiring FDG images (5). Although DHC has been used in nuclear oncology (6, 7), little has been reported about its application in neurologic brain FDG studies (8). The purpose of this study was to compare the clinical use of DHC with that of dedicated ring-detector PET (dr-PET) in a group of healthy volunteers and patients with various neurologic disorders.

Received March 19, 1999; accepted after revision August 4, 1999.

From the Departments of Radiology (K.Fukuc., K.H., K.Fukus., N.K., T.K., M.S., M.T., Y.I.) and Internal Medicine (H.M.), National Cardiovascular Center, Osaka, Japan.

Address reprint requests to Kohei Hayashida, MD, PhD, Department of Radiology, National Cardiovascular Center, Fujishiro-dai 5-7-1, Suita, Osaka 565-8565, Japan.

Methods

Subject Population

Seven healthy male volunteers (38 ± 5 years of age) and 12 patients with intracerebral lesions (eight men and four women; mean age, 62 ± 14 years; range, 29 to 84 years) underwent dr-PET followed by DHC imaging. All participants except the healthy volunteers had been assessed with the use of various techniques, including brain single-photon emission CT (SPECT) with ^{99m}Tc-HMPAO, CT, and MR imaging (Table 1). The health status of the volunteers was defined after medical review confirmed no history of cerebral disease. Written informed consent, in keeping with ethical guidelines established by the National Cardiovascular Center, was obtained from all participants.

Imaging Protocol

Study participants fasted for over 5 hours before dr-PET transmission scans were obtained using a line source of ^{68}Ga/^{68}Ge to correct for photon attenuation. FDG (approximately 185 MBq) was then administered and, 40 minutes later, emission imaging proceeded for 10 minutes. The dr-PET camera was an ECAT EXACT 47 (Siemens, Knoxville, TN) with a 16.2-cm axial field of view (9). Forty-seven axial attenuation-corrected slices each 2.0-mm thick in a 128 × 128 matrix were reconstructed using a Hanning filter (cutoff frequency, 1.25 cycles/cm).

TABLE 1: Clinical summary of the patients

Case	Age (y)/Sex	Clinical Characteristics	MR or CT Findings	No. of Studies
1	59/M	Alzheimer type dementia	Lacnar infarction	1
2	58/M	Primary brain tumor (mixed glioma)	L temporal mass	1
3	29/M	Cerebral embolism	L temporooccipital low-density area	1
4	62/M	Hemorrhagic infarction	R temporal hemorrhagic infarction	1
5	74/F	Cardiogenic embolism	L frontal low-density area Dilatation of lateral ventricle	1
6	60/M	Epilepsy	Periventricular hyperintensity	1
7	47/M	Cerebral embolism, epilepsy	L temporoparietal low-density area	1
8	57/F	Subarachnoid hemorrhage (postop), epilepsy	L frontotemporal low intensity	1
9	84/F	Metastatic brain tumor	L parietal mass + peripheral edema	1
10	67/M	Cerebral infarction	R frontoparietal low-density area	1
11	71/M	Brain injury, epilepsy	L temporoparietal damage	3
12	74/F	Brain abscess	R occipital mass	1

DHC imaging was performed 90 to 100 minutes after FDG injection, according to the DHC acquisition protocol. Sixty-four projections of coincidence detection were obtained at 40 seconds per projection every 5.6° for 360° (180° × 2), in a 128 × 128 matrix. Frame-by-frame decay correction was performed before image reconstruction using a Butterworth filter (cut-off frequency 1.20 cycles/cm, order 10). Chang's postreconstruction attenuation correction was applied to the axial slices by fitting an ellipse to the scalp contour for the entire brain with an attenuation coefficient of 0.08 cm^{-1} (10). The final reconstructed axial image was generated from 2.0-mm-thick slices. The DHC was a VERTEX Plus MCD (ADAC Laboratories, Milpitas, CA). With coincidence detection where the timing window between the two detectors was set to 15 nsec, only about 1% of the single detector counts corresponded to true coincidence events (6).

Data Analysis

The normal FDG uptake as seen on the DHC and dr-PET images from seven healthy volunteers was evaluated using six corresponding axial scans to define anatomic levels (+16-, +24-, +32-, +40-, +48-, and +64-mm planes parallel to the canthomeatal line) for semiquantitative analysis (11). Twenty-two brain regions (>100 pixels) including right and left sides were manually placed on appropriately matched scans by visual inspection and by means of a generalized template modified from the brain atlas of Matsui and Hirano (12). Individual cortical regions were combined into inferior frontal, superior frontal, anterior temporal, posterior temporal, anterior cingulate, parietal, and occipital cortices. Additional regions of interest (ROIs) were placed in the thalamus, basal ganglia (caudate nucleus), and cerebellum. The data obtained by placing ROIs included the mean counts per pixel. Relative FDG uptake was calculated for each ROI by using the average tissue activity in the region standardized by mean cerebellar hemispheric activity.

In addition, we compared the data from seven healthy volunteers and 14 studies of 12 patients to obtain correlation coefficients between cerebral FDG accumulation in the DHC and dr-PET images. A total of 14 new ROIs were selected from the frontal, temporal, parietal, and occipital areas of the cortex, and from the thalamus, basal ganglia, and cerebellum bilaterally on axial slices, and the mean counts per voxel were estimated in each ROI with reference to an anatomic map (13). Average counts per pixel of each cortical area were then divided by the average counts per pixel found in the cerebellar hemispheric activity.

Statistical Analysis

DHC and dr-PET results were compared using Student's *t*-test for paired samples. Correlations were determined by linear regression analysis. A probability level below .05 was considered to indicate a significant difference.

Results

Representative axial DHC and dr-PET images from a healthy volunteer are shown in Figure 1. Both sets of images clearly show brain FDG distribution, but the image contrast with DHC is lower than that with dr-PET. FDG uptake in the frontal lobe was relatively higher with DHC imaging as compared with that of dr-PET.

The results of the ROI analysis of the FDG distribution between DHC and dr-PET in seven volunteers are shown in Table 2. No significant differences between the two sets of images were evident in the temporal, parietal, or occipital cerebral lobes. The level of FDG in the superior frontal cortex was increased, however, and uptake in the thalamus was significantly decreased with DHC as compared with dr-PET.

In the visual assessment of the patients, all abnormal lesions that were seen with dr-PET were detected with DHC imaging. Figure 2 shows images of a patient with Alzheimer-type dementia that demonstrate decreased FDG uptake in the bilateral temporoparieto-occipital region on both DHC and dr-PET images. In a patient with brain injury and symptomatic epilepsy, DHC images revealed multiple lesions of increased FDG accumulation in the right cerebral cortices and the basal ganglia with the same clarity as on the dr-PET scans (Fig 3). Scalp EEG confirmed that the focus of epilepsy was located in the right superior frontal cortex.

The results of a quantitative comparison of FDG distribution between DHC imaging and dr-PET in 252 regions of the 14 patients and the seven healthy volunteers are shown in Figure 4. The cerebrum/cerebellum ratio of each cerebral region on DHC and dr-PET images was significantly correlated and agreed well (DHC = 0.85 × dr-PET + 0.20; r = .86, $P < .0001$).

Discussion

Our results showed some difference between DHC imaging and dr-PET, but this difference ap-

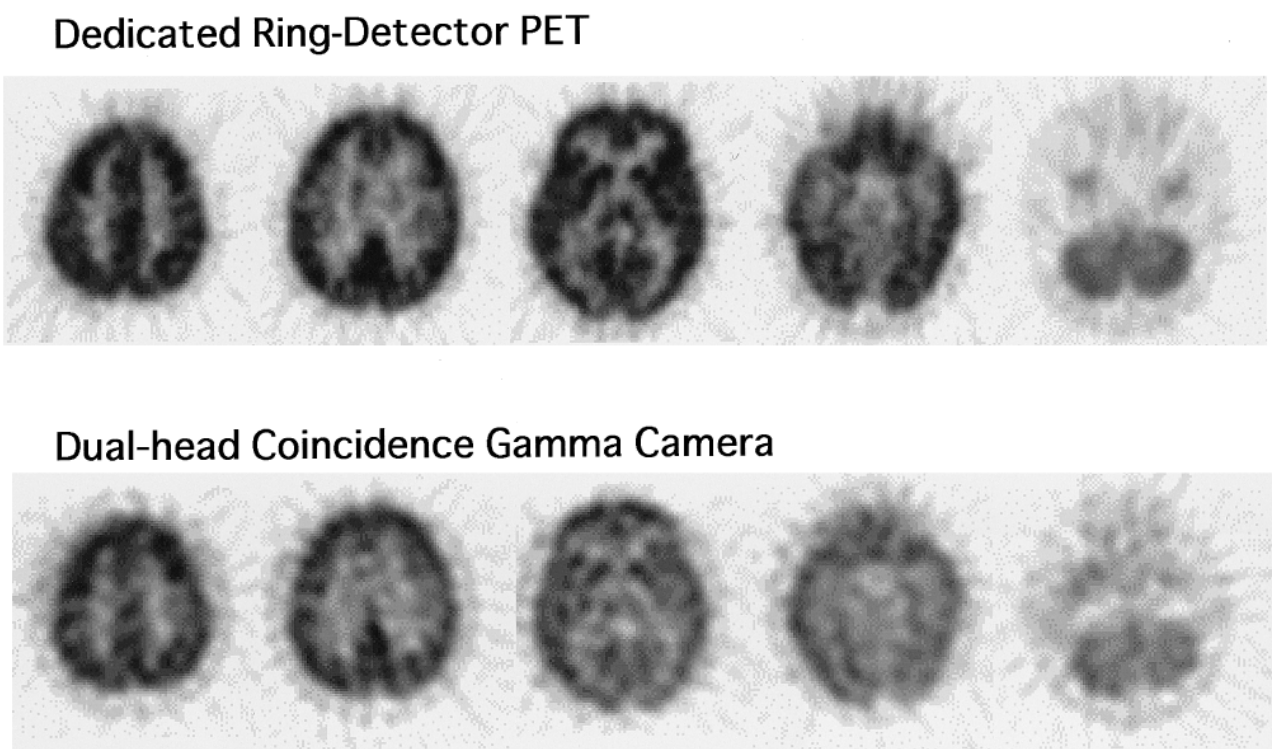

FIG 1. Comparison of FDG images obtained from a healthy volunteer using dedicated ring-detector PET (dr-PET) (*upper panel*) and a dual-head coincidence gamma camera (DHC) (*lower panel*). Both sets of images clearly show brain FDG distribution, but the contrast with DHC was lower than that with dr-PET. FDG uptake in the frontal lobe was relatively higher with DHC as compared with that of dr-PET.

TABLE 2: Relative regional FDG uptake: regional average/cerebellum

Region	Dedicated Ring-Detector PET	Dual-Head Coincidence Gamma Camera	*P* Value
Anterior cingulate	1.30 ± 0.09	1.36 ± 0.08	.142
Inferior frontal cortex	1.22 ± 0.13	1.20 ± 0.09	.631
Superior frontal cortex	1.29 ± 0.09	1.50 ± 0.07	.003
Anterior temporal cortex	1.10 ± 0.13	1.17 ± 0.05	.213
Posterior temporal cortex	1.16 ± 0.11	1.14 ± 0.05	.525
Parietal cortex	1.21 ± 0.16	1.31 ± 0.11	.180
Occipital cortex	1.27 ± 0.11	1.37 ± 0.07	.064
Caudate nuclei	1.29 ± 0.10	1.26 ± 0.06	.502
Thalamus	1.13 ± 0.06	1.01 ± 0.13	.034

pears to be negligible for semiquantitative assessment. Thus, DHC as well as dr-PET techniques may be used to map regional cerebral glucose distribution and may be widely applicable in the evaluation of intracerebral diseases.

Clinical indications for brain FDG imaging have been evaluated, with the results generating the following conclusions: FDG-PET is useful for defining the degree of malignancy and for differentiating recurrent tumors from necrosis after therapy in patients with brain tumors (2, 14). FDG-PET studies have been performed in epileptic patients to detect and localize epileptic foci. These studies have been verified by scalp EEG, MR imaging, site of surgery, and clinical outcome (1, 15). In addition, FDG-PET is routinely used to detect cerebral metabolic reduction in neuropsychological disorders (3, 16). These clinical results with dr-PET have accelerated interest in applying FDG imaging to the evaluation of cerebral disease.

FDG can be imaged using either a conventional SPECT device with an ultra high-energy collimator for 511-keV photons (FDG-SPECT) or a DHC, which has two key advantages over the former: the sensitivity of DHC is 10 times higher than that of SPECT and the spatial resolution is 6 mm compared with the 15 mm or so with FDG-SPECT (5, 6). Although FDG-SPECT has been somewhat successful in cardiac viability studies (17, 18), its low sensitivity and spatial resolution do not guarantee optimal results for brain and whole-body tumor imaging (19). Owing to these limitations, brain FDG-SPECT has not been enthusiastically tested. Thus, the question of whether brain FDG imaging with DHC can be an effective alternative to dr-PET is of considerable interest to neuroradiologists.

In a preliminary oncologic report, DHC was clearly inferior to dr-PET because of a lack of attenuation correction and higher background activity (6); however, brain DHC has some advantages in whole-body studies. Because the brain is thought to be homogeneously attenuated, mathematical uniform attenuation correction in brain studies is more reliable than that in whole-body studies that have patient-specific attenuation artifacts (10). DHC was

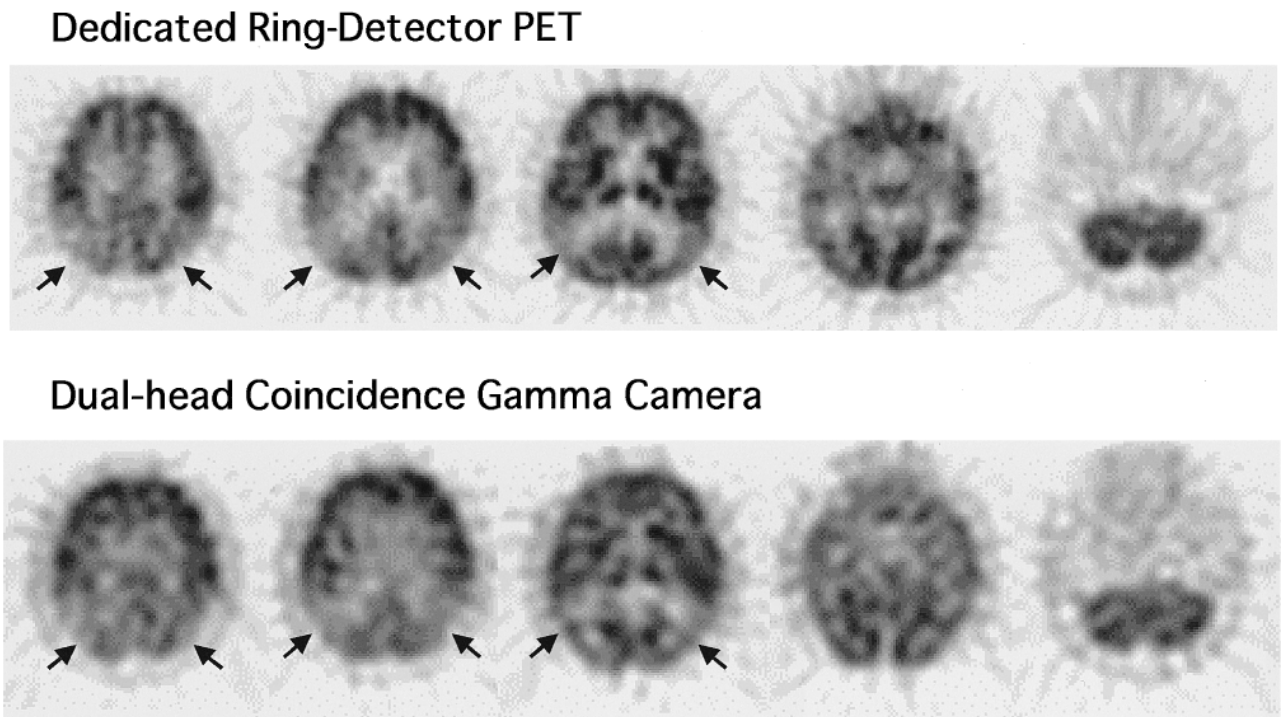

FIG 2. 59-year-old man with Alzheimer-type dementia. Dedicated ring-detector PET (dr-PET) images (*upper panel*) show reduced uptake in both temporoparieto-occipital regions with no other sites of reduced uptake. Dual-head coincidence gamma camera images (*lower panel*) show reduced uptake in bilateral temporoparieto-occipital regions as well as the dr-PET images do.

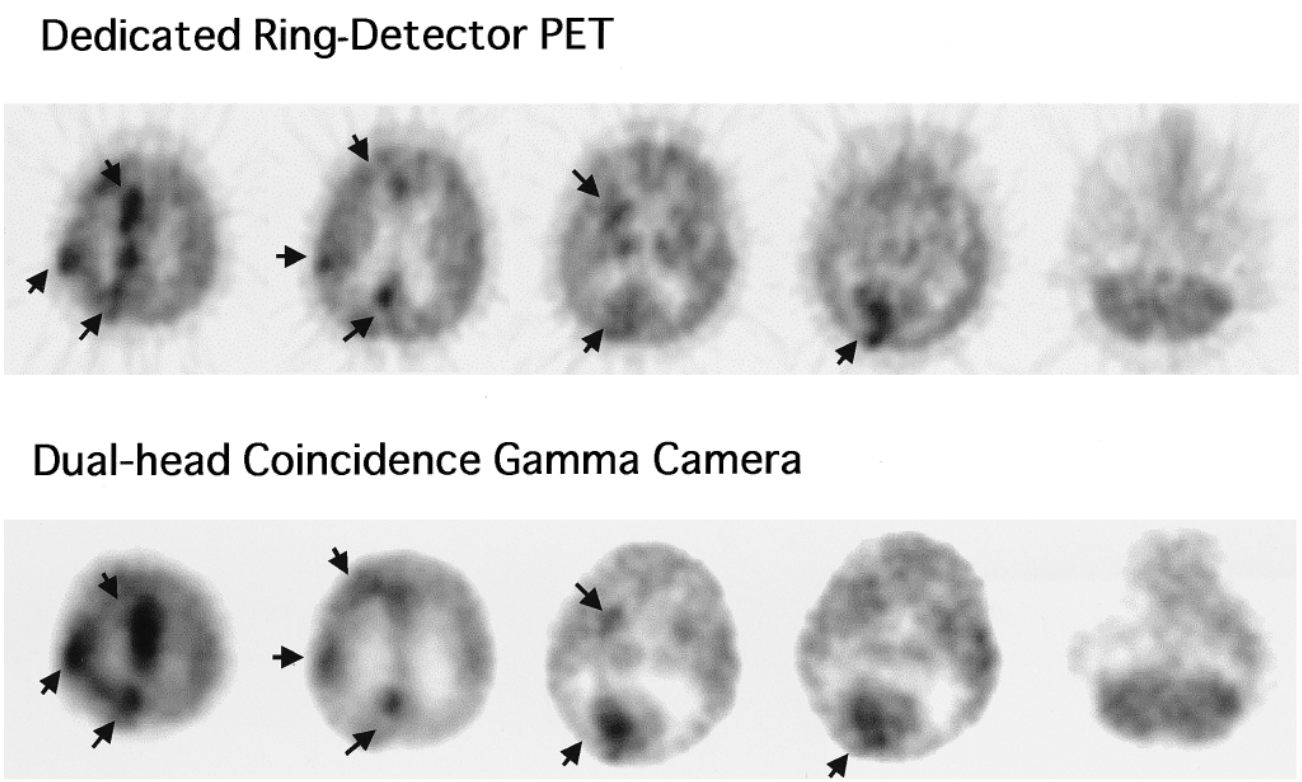

FIG 3. 71-year-old man with post-traumatic epilepsy. Dedicated ring-detector PET images (*upper panel*) show multiple lesions of increased FDG accumulation in the right cerebral cortices and basal ganglia. Dual-head coincidence gamma camera images (*lower panel*) also show multiple lesions of increased FDG accumulation.

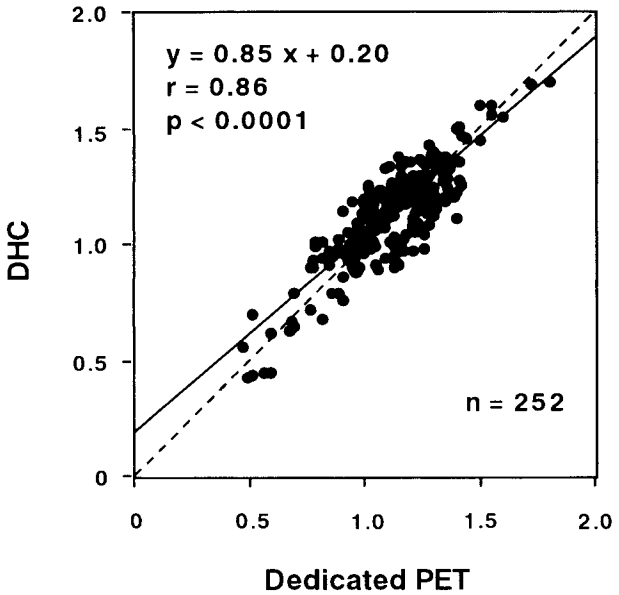

FIG 4. Comparison of FDG uptake ratios between dual-head coincidence gamma camera (DHC) imaging and dedicated ring-detector PET (dr-PET) in 252 regions of 21 subjects. The cerebrum/cerebellum ratio in DHC imaging revealed a close relationship with that of dr-PET.

corrected for attenuation artifacts using mathematical uniform attenuation correction, whereas dr-PET images were corrected using transmission-based nonuniform attenuation correction. The mathematical procedure is not sufficiently accurate to correct photon attenuation in theory. In addition, Chang's attenuation correction can be performed by fitting only a single ellipse with the software in our coincidence-capable gamma camera system. It is well recognized that using a single ellipse will cause an error in attenuation correction, since the head contour varies from slice to slice. Nevertheless, despite some shortcomings of the methods of attenuation correction in the DHC study, brain DHC revealed a similar semiquantitative FDG distribution to dr-PET images obtained in patients with a variety of cerebral diseases, thus confirming the clinical feasibility of DHC in evaluating brain glucose metabolism. The diagnostic value of this technology should be compared with that of dr-PET using a large study population.

The present study of healthy volunteers showed that the cerebral FDG distribution in DHC images was a little different from that of dr-PET. This discrepancy could be ascribed to the acquisition systems involved, the physical features of the technologies, or the means of data processing. One explanation pertains to the methodological difference in attenuation correction between DHC and dr-PET alluded to previously. Another unavoidable factor that creates a discrepancy between DHC and dr-PET findings is the scatter fraction. We used a 2D acquisition mode in the present dr-PET study, whereas DHC acquisition was essentially in a 3D mode (5). A large increase in the scatter fraction of the measured coincidence events is a major problem in quantitative 3D data acquisition. PET studies using a 3D mode show apparently decreased image contrast as compared with 2D dr-PET studies (20). DHC uses sodium iodide crystals, which give a better energy resolution than those of the bismuth germinates that are commonly used for dr-PET scanning. DHC, however, has the same potential as 3D dr-PET for scatter fraction problems, because it does not use lead septa, like 2D dr-PET. The higher counts in the superior frontal area and the lower counts in the thalamus on DHC studies might be due to a relatively large variation in attenuation correction and scatter fraction between slices through the basal ganglia and those through the superior frontal cortex.

Another potential limitation of our study was that DHC imaging was done about 1 hour after the dr-PET study to permit both types of imaging on the same day without subjecting the participants to increased exposure. FDG uptake in the myocardium and in tumors increases over time, and delayed FDG images may differ from those acquired 40 minutes after injection (21, 22). One study, however, has indicated that a single FDG brain scan of healthy volunteers at any time from 60 to 120 minutes after tracer injection is optimal (23). Thus, we considered that the difference between the two imaging techniques was not due to acquisition timing.

Conclusion

Considering the differences in the physical performance and the data processing technology between DHC imaging and dr-PET, DHC with FDG has a potential to image brain FDG distribution that is almost equal to that of dr-PET. Thus, DHC with FDG may be used to evaluate intracranial disease instead of the more expensive dr-PET system.

Acknowledgments

We thank Yoshinori Miyake and the cyclotron staff for technical support with the production of ^{18}F-FDG, Takashi Nishihara and Hisashi Oka for skilled imaging, and Norma Foster for critical reading of the manuscript.

References

1. Coubes P, Awad IA, Antar M, Magdinec M, Sufka B. **Comparison and spatial correlation of interictal HMPAO-SPECT and FDG-PET in intractable temporal lobe epilepsy.** *Neurol Res* 1993;15:160–168
2. Buchpiguel CA, Alavi JB, Alavi A, Kenyon LC. **PET versus SPECT in distinguishing radiation necrosis from tumor recurrence in the brain.** *J Nucl Med* 1995;36:159–164
3. Weinstein HC, Scheltens P, Hijdra A, van Royen EA. **Neuro-imaging in the diagnosis of Alzheimer's disease, II: positron and single photon emission tomography.** *Clin Neurol Neurosurg* 1993;95:81–91
4. Conti PS, Keppler JS, Halls JM. **Positron emission tomography: a financial and operational analysis.** *AJR Am J Roentgenol* 1994; 162:1279–1286
5. Jarritt PH, Acton PD. **PET imaging using gamma camera systems: a review.** *Nucl Med Commun* 1996;17:758–766
6. Shreve P, Steventon R, Deters E, Kison P, Gross M, Wahl R. **Oncologic diagnosis with 2-[fluorine-18]fluoro-2-deoxy-D-glucose**

imaging: dual-head coincidence gamma camera versus positron emission tomographic scanner. *Radiology* 1998;207: 431–437
7. Stokkel MP, Terhaard CH, Mertens IL, Hordijk G, van Rijk PP. **Fluorine-18-FDG detection of laryngeal cancer postradiotherapy using dual-head coincidence imaging.** *J Nucl Med* 1998;39:1385–1387
8. Delbele D, Patton JA, Martin WH, Sandler MP. **FDG PET and dual-head gamma camera positron coincidence detection imaging of suspected malignancies and brain disorders.** *J Nucl Med* 1999;40:110–117
9. Wienhard K, Eriksson L, Grootoonk S, Casey M, Pietrzyk U, Heiss WD. **Performance evaluation of the positron scanner ECAT EXACT.** *J Comput Assist Tomogr* 1992;16:804–813
10. Chang L. **A method for attenuation correction in radionuclide computed tomography.** *IEEE Trans Nucl Sci* 1978;NS-25: 638–643
11. Mayberg HS, Lewis PJ, Regenold W, Wagner HN. **Paralimbic hypoperfusion in unipolar depression.** *J Nucl Med* 1994;35: 929–934
12. Matsui T, Hirano A. ***An Atlas of the Human Brain for Computerized Tomography.*** Tokyo: Igaku-Shoin; 1978
13. Kume N, Hayashida K, Cho IH, Shimotsu Y, Nishioeda Y, Matsunaga N. **Visualization of frontal postural hypoperfusion in patients with Takayasu arteritis with upright 99mTc-HMPAO brain SPECT.** *Nucl Med Commun* 1997;18:943–950
14. Colemann RE, Hoffman JM, Hanson MW, Sostman HD, Schold SC. **Clinical application of PET for the evaluation of brain tumors.** *J Nucl Med* 1991;32:616–622
15. Fisher RS, Frost JJ. **Epilepsy.** *J Nucl Med* 1991;32:651–659
16. Minoshima S, Foster NL, Kuhl DE. **Posterior cingulate cortex in Alzheimer's disease.** *Lancet* 1994;344:–895
17. Martin WH, Delbeke D, Patton JA, et al. **FDG-SPECT: correlation with FDG-PET.** *J Nucl Med* 1995;36:988–995
18. Chen EQ, MacIntyre WJ, Go RT, et al. **Myocardial viability studies using fluorine-18-FDG SPECT: a comparison with fluorine-18-FDG PET.** *J Nucl Med* 1997;38:582–586
19. Drane WE, Nicole MW, Mastin ST, Kuperus JH. **SPECT with 2-[fluorine-18]fluoro-2-deoxy-D-glucose (FDG).** *Radiology* 1995; 197:341–342
20. Cherry SR, Dahlbom M, Hoffman EJ. **3D PET using a conventional multislice tomograph without septa.** *J Comput Assist Tomogr* 1991;15:655–66
21. Srinivasan G, Bacharach SL, Kitsiou AN, Nour KA, Davis CM, Dilsizian V. **Delayed FDG imaging improves myocardial/blood pool contrast (abstr).** *J Am Coll Cardiol* 1997;29:–436A
22. Hamberg LM, Hunter GJ, Alpert NM, Choi NC, Babich JW, Fischman AJ. **The dose uptake ratio as an index of glucose metabolism: useful parameter or oversimplification?** *J Nucl Med* 1994;35:1308–1312
23. Lucignani G, Schmidt KC, Moresco RM, et al. **Measurement of regional cerebral glucose utilization with fluorine-18-FDG and PET in heterogeneous tissues: theoretical considerations and practical procedure.** *J Nucl Med* 1993;34:360–369